

Bonding and Disorder in Liquid Silicon

I. Štich,⁽¹⁾ R. Car,⁽¹⁾ and M. Parrinello^(1,2)

⁽¹⁾International School for Advanced Studies, Strada Costiera 11, Trieste 34014, Italy

⁽²⁾IBM Research Division, Forschungslaboratorium Zürich, Rüschlikon 8803, Switzerland

(Received 21 July 1989)

A first-principles molecular-dynamics study of metallic liquid silicon is presented. Our description of the local order is in excellent agreement with x-ray and neutron diffraction experiments. Analysis of the electronic charge density shows persistence of some covalent chemical bonds in the liquid. These bonds give rise in the power spectrum of the system dynamics to a well identifiable feature associated with stretching vibrations. The single-particle electronic density of states shows metallic behavior. The calculated electronic conductivity agrees well with the available experimental information.

PACS numbers: 61.20.Ja, 61.25.Mv, 71.25.Lf, 72.15.Cz

The prototype elemental semiconductor Si in its liquid state has several intriguing and poorly understood properties. Upon melting it goes from a fourfold semiconducting structure to a metallic low coordinated liquid.¹ In the liquid metallic phase the density is $\sim 10\%$ higher than that of the solid² and the structure factor is dissimilar to that of most liquid metals. The average coordination number from the experimental pair correlation function is between 6 and 7,^{3,4} depending on the definition, while most liquid metals are closely packed with a coordination ranging from ~ 12 to 14. The low coordination of liquid silicon (*l*-Si) indicates a persistence of covalent bonding in the liquid. However, no quantitative description of such effects has so far been provided. It is a challenge of modern liquid state theories to reconcile the persistence of covalent bonding with metallic behavior and fast diffusion.

Theoretical efforts have mostly focused either on reproducing the experimental ionic structure by the use of effective classical potentials⁵ or on studying the electronic properties for a given model for the ionic structure.⁶ Both approaches miss the close connection between electronic and ionic structures. For this reason we have used here an *ab initio* molecular-dynamics (MD) method⁷ in which the interatomic forces are calculated from an accurate local-density approximation (LDA)⁸ electronic ground state. Without adjustable parameters we find results that are in close agreement with the experimental data. By analyzing the electronic charge density we infer that covalent chemical bonds persist in the liquid. However, the majority of bonds are broken leading to diffusive and metallic behavior.

We have performed a constant-temperature-constant-volume MD simulation at the experimental density $\rho = 2.59 \text{ g cm}^{-3}$ (Ref. 2) and at temperature $T = 1800 \text{ K}$, close to the experimental melting point of $\sim 1680 \text{ K}$. In order to fix the ionic temperature we followed Nosé's⁹ prescription and introduced in the equations of motion of Ref. 7 an additional dynamical variable s , acting as a thermostat on the ionic degrees of freedom. The resulting

equations of motion are

$$\mu \frac{d^2}{dt^2} \psi_i(\mathbf{r}, t) = - \frac{\delta E}{\delta \psi_i^*(\mathbf{r}, t)} + \sum_j \Lambda_{ij} \psi_j(\mathbf{r}, t), \quad (1a)$$

$$M_I \frac{d^2}{dt^2} \mathbf{R}_I = - \frac{\partial E}{\partial \mathbf{R}_I} - \frac{M_I}{s} \frac{d\mathbf{R}_I}{dt} \frac{ds}{dt}, \quad (1b)$$

$$Q \frac{d^2}{dt^2} s = s \sum_I M_I \left(\frac{d\mathbf{R}_I}{dt} \right)^2 - s g k_B T + \frac{Q}{s} \left(\frac{ds}{dt} \right)^2. \quad (1c)$$

Here Q is a dynamical mass associated to the thermostat, k_B is Boltzman's constant, T is the desired ionic temperature, and $g = 3N$, where N is the number of atoms in the simulation box. As demonstrated by Nosé, Eqs. (1b) and (1c) lead to a canonical distribution in the ionic phase space.

In the present simulation we used norm-conserving pseudopotentials¹⁰ with s nonlocality only. Kleinman and Bylander's factorized form¹¹ was adopted to speed up the calculation. Exchange and correlation effects were treated within LDA.¹² The Γ point only was used to sample the Brillouin zone (BZ) of the MD supercell, containing 64 atoms with periodic boundary conditions of the simple cubic (sc) type. The electronic orbitals were expanded in plane waves. The integration time step for the equations of motion was 5.5 a.u. ($1.3 \times 10^{-16} \text{ s}$), the fictitious mass μ was taken to be 300 a.u., and Q was set to 2.5×10^5 a.u. In the insulating Si phases this choice would have insured very accurate adiabaticity for times of the order of a few picoseconds. In the liquid metallic phase the system remains very close to the Born-Oppenheimer surface only for times longer than 500 time steps. Therefore periodic quenches of the electrons to the instantaneous ground state were performed every 500 time steps in order to guarantee strict adiabatic evolution. Use of the Nosé thermostat keeps the average ionic temperature constant and equal to T , despite the small but continuous energy transfer from ions to the electronic degrees of freedom. Notice that within our approach one neglects thermal effects on the electronic

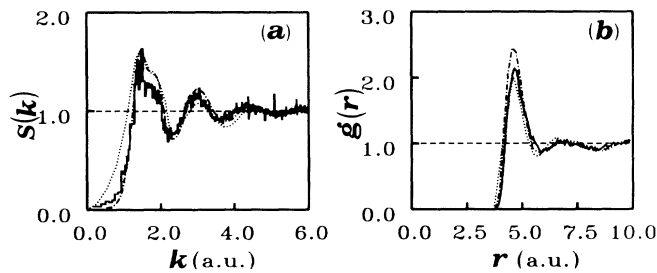


FIG. 1. (a) Static structure factor and (b) pair correlation function. Full line, MD simulation; dotted line, neutron diffraction experiment (Ref. 4); dash-dotted line, x-ray diffraction experiment (Ref. 3).

Fermi surface, which is assumed to be perfectly sharp as at $T=0$ K. This is justified since, at the temperatures of the simulation, the thermal smearing of the Fermi surface is small compared with the occupied valence bandwidth. After equilibration we have followed the system for a total time of 1.2 ps, much larger than the typical relaxation times.

We have checked the convergence of our calculation with respect to periodic boundary conditions, cell size, inclusion of p nonlocality in the pseudopotential, and energy cutoff in the plane-wave expansion of the electronic wave functions. The results were quite sensitive to variations in the energy cutoff, while changes in other conditions produced only minor effects. A cutoff of 12 Ry was necessary to achieve convergence and produce a coordination in close agreement with experiments. By lowering the cutoff we observed a reduced tendency toward metalization and a simultaneous trend toward more structured systems having lower average coordination. In particular, with an energy cutoff of ~ 6 Ry we reproduced, with the 64-atom sc cell, the results already found in a preliminary calculation done with a 54-atom fcc cell and similar cutoff.¹³ The observed relative independence of the structural properties on the unit-cell size and shape provides an indication that the calculation of the interatomic forces, which requires a BZ average, is essentially well converged with respect to k -point sampling.

In Fig. 1 we show the results obtained for the static structure factor $S(k)$ and the pair correlation function $g(r)$. Comparison with x-ray³ and neutron scattering⁴ experiments is very favorable, especially if one considers the difference between the two sets of experimental data and the absence of any fitting parameter in the theory. The coordination number, as obtained by integrating $g(r)$ up to the first minimum $r_m = 5.85$ a.u., is ~ 6.5 in close agreement with the experimental value of ~ 6.4 .^{3,4} More details on the structure of the melt can be obtained from the bond-angle distribution function $g_3(\theta, r_m)$. Here θ is the angle between the two vectors that join a central particle with two neighbors at a distance less

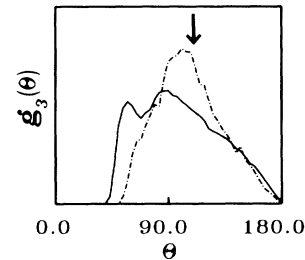


FIG. 2. Bond-angle distribution functions $g_3(\theta, r)$. The cutoff distance r is equal to r_m , the first minimum of $g(r)$ (full line), and to the covalent cutoff r_c defined in the text (dash-dotted line). The arrow indicates the position of the tetrahedral angle.

than r_m . Our $g_3(\theta, r_m)$ shown in Fig. 2 is rather broad with maxima centered at $\theta \sim 60^\circ$ and $\sim 90^\circ$. The broad nature of this distribution shows that it is not very useful to interpret the local order of l -Si in terms of the high-pressure metallic phases of crystalline Si (c -Si), like β -tin or simple cubic.

The vibrational density of states of the liquid can be obtained from the power spectrum of the velocity autocorrelation function $Z(t) = \frac{1}{3} \langle \mathbf{v}(0) \cdot \mathbf{v}(t) \rangle$. $Z(\omega)$ and the corresponding $Z(t)$ are shown in Fig. 3. $Z(t)$ is always positive and has an oscillatory decay to zero after ~ 0.15 ps. This has to be contrasted with close-packed liquids like Ar where a negative oscillation in $Z(t)$ is observed. This is believed to result from the caging effect of the shell of neighboring atoms.¹⁴ l -Si is a much more open structure and exhibits no caging but only a milder effect due to the occasional formation of covalent bonds between pairs of atoms. The bonding effects are reflected in the shoulder of $Z(\omega)$ at the frequency of ~ 40 meV, which is very close to the optical vibrational frequency of crystalline Si just below the melting point.¹⁵ From $Z(\omega)$ at $\omega=0$ we extract a self-diffusion coefficient $D \sim 2.0 \times 10^{-4} \text{ cm}^2 \text{ s}^{-1}$. Although we are not aware of any direct experimental measurement of D for l -Si, our finding is consistent with indirect estimates. In fact, one can compare D with the diffusivity of substantial impurities, such as P (Ref. 16) or use the Einstein's relation to deduce D from the measured viscosity.¹⁶

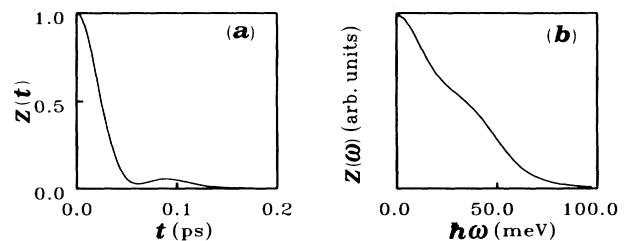


FIG. 3. (a) The velocity autocorrelation function and (b) the corresponding power spectrum.

Considerable insight into the bonding properties is obtained from a study of the valence electronic charge density $\rho_e(\mathbf{r})$. A plot of $\rho_e(\mathbf{r})$ in a plane defined by three neighboring atoms in the liquid is shown in Fig. 4 where for comparison we also report $\rho_e(\mathbf{r})$ in the (110) plane of *c*-Si. The two $\rho_e(\mathbf{r})$ have several common characteristics. In both cases the charge density is strongly nonuniform and there is an accumulation of charge density between pairs of adjacent atoms. Figure 4 provides striking evidence for the persistence of covalent bonds in the liquid. Figure 4(b) shows a snapshot of an instantaneous local configuration which changes in time with the typical time scale of the diffusive motion of the atoms. Its subsequent evolution at intervals of time of ~ 0.02 ps is shown in Figs. 4(c) and 4(d). We notice that in Fig. 4(c) one of the two bonds of Fig. 4(b) starts to break, while the other is substantially weakened.

Finally, in Fig. 4(d) both bonds have disappeared, while in the upper left corner one can see the formation of a new bond with an incoming atom not shown in the picture. An extensive analysis shows that covalent bonds almost always form between pairs separated by a distance less than ~ 4.7 a.u. For larger separation distances the great majority of the bonds are broken. We can therefore define $r_c = 4.7$ a.u. as the cutoff distance for covalent bonds. This is slightly larger than the equilibrium bond length of 4.44 a.u. of *c*-Si. Only a fraction of $\sim 30\%$ of the atoms in the first peak of $g(r)$ are at distances less than r_c . The bond-angle distribution $g_3(\theta, r_c)$ corresponding to these atoms is shown in Fig. 2. $g_3(\theta, r_c)$ is peaked around an angle close to tetrahedral ($\theta \sim 109^\circ$). A similar albeit considerably narrower

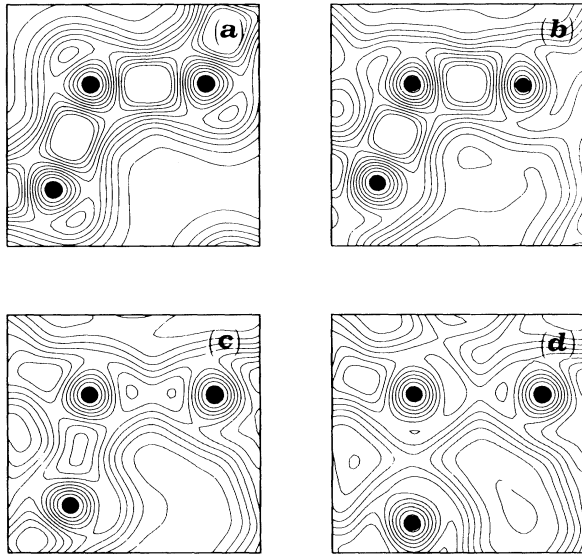


FIG. 4. Contour plots of the valence electronic density $\rho_e(\mathbf{r})$. (a) *c*-Si in the (110) plane. (b)–(d) evolution of $\rho_e(\mathbf{r})$ in *l*-Si at time intervals of ~ 0.02 ps.

bond-angle distribution is found in amorphous silicon. The previous analysis demonstrates the presence in *l*-Si of fluctuations toward local tetrahedral order.

In Fig. 5(a) we report the single-particle electronic density of states $N(E)$, calculated by averaging the occupied and unoccupied density of states over twelve selected ionic configurations generated by MD and well separated in time. In the same figure we also report the density of occupied electronic states averaged over the entire MD run. The comparison shows that, at least for the occupied states, the twelve configurations provide a sufficiently representative sample. $N(E)$ displays metallic behavior as evidenced by the absence of a gap at the Fermi energy E_F . The finite-energy resolution of the histogram is a direct consequence of the small size of our simulation box. We have also calculated the electrical conductivity $\sigma(\omega)$ by means of the Kubo-Greenwood (KG) formula¹⁸

$$\sigma(\omega) = \frac{2\pi e^2}{\Omega m^2} \sum_{i,j} \frac{|M_{ij}|^2}{\omega_{ji}} \delta(\epsilon_j - \epsilon_i - \hbar\omega), \quad (2)$$

where M_{ij} is the momentum-operator matrix between states $|i\rangle, |j\rangle$. The result is shown in Fig. 5(b). By extrapolating the calculated conductivity to $\omega \rightarrow 0$, we obtain $\sigma_{dc} = 0.38$ a.u. [$0.0175 (\mu\Omega \text{ cm})^{-1}$] in fairly good agreement with the experimental value of 0.27 a.u. [$0.0124 (\mu\Omega \text{ cm})^{-1}$].^{1,17} An alternative estimation of σ_{dc} can be obtained from the appropriate expression¹⁹

$$\sigma_{dc} = \frac{4\pi^2 \hbar^3 e^2}{3m^2} a [N(E_F)]^2, \quad (3)$$

where a is the average nearest-neighbor distance. This gives $\sigma_{dc} = 0.18$ a.u. [$0.0083 (\mu\Omega \text{ cm})^{-1}$] in reasonable agreement both with the KG expression and with experimental data.

In conclusion, we have performed a first-principles study of *l*-Si. On the whole our results are in excellent

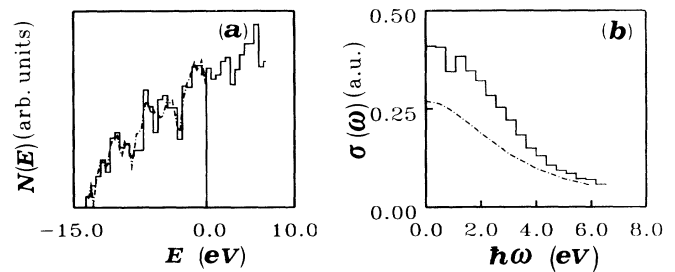


FIG. 5. (a) Single-particle electronic density of states. Full line, average over twelve ionic configurations; dash-dotted line, average over the entire MD trajectory. The vertical line indicates the position of the Fermi energy E_F . (b) Electrical conductivity from the Kubo-Greenwood formula. The dash-dotted line indicates a Drude fit to the measured experimental data (Ref. 17). The atomic unit of conductivity used here is $e^2/\hbar a_B = 4.6 \times 10^6 (\Omega \text{ m})^{-1}$.

agreement with experimental data for both structural and electronic properties. In particular, we have given a quantitative theoretical basis to the concept of covalent effects in metallic *l*-Si by identifying some peculiar fluctuations toward local tetrahedral order. Such fluctuations may play an important role in explaining why silicon is able to reconstruct easily a tetrahedral network upon cooling.

This work has been supported by the Scuola Internazionale Superiore di Studi Avanzati-Centro di Calcolo Elettronico Interuniversitario dell'Italia Nord-Orientale collaborative project, under the sponsorship of the Italian Ministry for Public Education. Two of us (R.C. and M.P.) acknowledge support from the European Research Office of the U.S. Army.

¹V. M. Glazov, S. N. Chizhevskaya, and N. N. Glagoleva, *Liquid Semiconductors* (Plenum, New York, 1969).

²Y. Waseda, *The Structure of Non-Crystalline Materials: Liquids and Amorphous Solids* (McGraw-Hill, New York, 1980).

³Y. Waseda and K. Suzuki, *Z. Phys.* B **20**, 339 (1975).

⁴J. P. Gabathuler and S. Steeb, *Z. Naturforsch.* **34a**, 1314 (1979).

⁵J. Hafner and G. Kahl, *J. Phys.* F **14**, 2259 (1984); F. H. Stillinger and T. A. Weber, *Phys. Rev. B* **31**, 5262 (1985); J. Q. Broughton and X. P. Li, *ibid.* **35**, 9120 (1987); M. D. Kluge, J. D. Ray, and A. Rahman, *ibid.* **36**, 4234 (1987); W. D. Luedtke and U. Landman, *ibid.* **37**, 4656 (1988).

⁶J. P. Gaspard, Ph. Lambin, C. M. Moutet, and J. P. Vigneron, *Philos. Mag.* B **50**, 103 (1984); P. B. Allen and J. Q. Broughton, *J. Phys. Chem.* **91**, 4964 (1987).

⁷R. Car and M. Parrinello, *Phys. Rev. Lett.* **55**, 2471 (1985).

⁸See, for instance, *Theory of the Inhomogeneous Electron Gas*, edited by S. Lundqvist and N. H. March (Plenum, New York, 1983).

⁹S. Nosé, *Mol. Phys.* **52**, 255 (1984); *J. Chem. Phys.* **81**, 511 (1984).

¹⁰G. B. Bachelet, D. R. Hamann, and M. Schlüter, *Phys. Rev. B* **26**, 4199 (1982).

¹¹L. Kleinman and D. M. Bylander, *Phys. Rev. Lett.* **48**, 1425 (1982).

¹²J. P. Perdew and A. Zunger, *Phys. Rev. B* **23**, 5048 (1981).

¹³R. Car and M. Parrinello, in *Proceedings of the Eighteenth International Conference on the Physics of Semiconductors, Stockholm, Sweden, 1986*, edited by O. Engstrom (World Scientific, Singapore, 1987), p. 1169.

¹⁴J. P. Hansen and I. R. McDonald, *Theory of Simple Liquids* (Academic, London, 1976), p. 180ff.

¹⁵C. Z. Wang, C. T. Chan, and K. M. Ho, *Phys. Rev. B* **39**, 8586 (1989).

¹⁶*Landolt-Börnstein: Numerical Data and Functional Relationship in Science and Technology*, edited by K.-H. Hellwege and O. Madelung (Springer-Verlag, Berlin, 1984), Group III, Vol. 17, Subvolume c.

¹⁷K. M. Shvarev, B. A. Baum, and P. V. Geld, *Fiz. Tverd. Tela (Lenigrad)* **16**, 3246 (1974).

¹⁸E. N. Economou, *Green's Functions in Quantum Physics*, Springer Series in Solid State Sciences Vol. 7 (Springer-Verlag, Berlin, 1983), p. 152ff.

¹⁹N. F. Mott and E. A. Davis, *Electronic Processes in Non-crystalline Materials*, The International Series of Monographs on Physics (Clarendon, Oxford, 1979), p. 182.